Electrospun polycaprolactone incorporated with fluorapatite nanoparticles composite scaffolds enhance healing of experimental calvarial defect on rats

Shasha He[1#^], Qihang Hu[1#], Yuting Sun[1], Yongxiang Xu[2], Lanzhu Huang[1], Gang Cao[3], Ting Guo[1]

[1]Department of General Dentistry, Nanjing Stomatological Hospital, Affiliated Hospital of Medical School, Nanjing University, Nanjing, China; [2]Department of Dental Materials, Peking University School and Hospital of Stomatology, Beijing, China; [3]Department of Stomatology, Jinling Hospital, Medical School of Nanjing University, Nanjing, China

Contributions: (I) Conception and design: T Guo, G Cao, S He, Q Hu; (II) Administrative support: T Guo, L Huang; (III) Provision of study materials or patients: T Guo, Y Xu; (IV) Collection and assembly of data: S He, Q Hu, Y Sun; (V) Data analysis and interpretation: S He, Q Hu, G Cao, T Guo; (VI) Manuscript writing: All authors; (VII) Final approval of manuscript: All authors.

[#]These authors contributed equally to this work.

Correspondence to: Ting Guo, PhD. Department of General Dentistry, Nanjing Stomatological Hospital, Affiliated Hospital of Medical School, Nanjing University, 30 Zhongyang Rd., Nanjing 210008, China. Email: Guoting_nj@126.com; Gang Cao, PhD. Department of Stomatology, Jinling Hospital, Medical School of Nanjing University, 305 Zhongshan East Rd., Nanjing 210002, China. Email: Caogang_nj@126.com.

Background: Composite scaffolds that maximize the advantages of different polymers are widely utilized in guided tissue regeneration (GTR). Some studies found that novel composite scaffolds composed of electrospun polycaprolactone/fluorapatite (ePCL/FA) actively promoted the osteogenic mineralization of various cell types *in vitro*. However, only a few studies have addressed the application of this composite scaffold membrane material *in vivo*. In this study, the ability of ePCL/FA composite scaffolds *in vivo* and their possible mechanisms were preliminarily explored.

Methods: In this study, ePCL/FA composite scaffolds were characterized and their effects on bone tissue engineering and repair of calvarial defects in rats were examined. Sixteen male Sprague-Dawley (SD) rats were randomly categorized into four groups: normal group (integral cranial structure without defect), control group (cranial defect), ePCL group (cranial defect repaired by electrospun polycaprolactone scaffolds), and ePCL/FA group (cranial defect repaired by fluorapatite-modified electrospun polycaprolactone scaffolds). At 1 week, 2 months, and 4 months, micro-computed tomography (micro-CT) analysis was performed to compare the bone mineral density (BMD), bone volume (BV), tissue volume (TV), and bone volume percentage (BV/TV). The effects of bone tissue engineering and repair were observed by histological examination (hematoxylin and eosin, Van Gieson, and Masson respectively) at 4 months.

Results: In water contact angle measurement, the average contact angle for the ePCL/FA group was significantly lower than that for the ePCL group, indicating that the FA crystal improved the hydrophilicity of the copolymer. Micro-CT analysis revealed that the cranial defect had no significant change at 1 week; however, the BMD, BV, and BV/TV of the ePCL/FA group were significantly higher than those of the control group at 2 and 4 months. Histological examination showed that the cranial defects were almost completely repaired by the ePCL/FA composite scaffolds at 4 months compared to the control and ePCL groups.

Conclusions: The introduction of a biocompatible FA crystal improved the physical and biological properties of the ePCL/FA composite scaffolds; thus, these scaffolds demonstrate outstanding osteogenic potential for bone and orthopedic regenerative applications.

^ ORCID: 0000-0002-2765-3795.

Page 2 of 14

He et al. Composite scaffolds promote calvarial defect healing

Introduction

Bone defects are ubiquitous conditions that severely impact the functionality and integrity of the oral-maxillary system, and they are often caused by inflammation, injuries, or tumors in the oral and maxillofacial regions. Despite bone tissue has the ability to regenerate itself, critical-size bony defects exceed the regeneration ability of the bone tissue and would require additional support (1). Guided bone regeneration (GBR) is a promising approach for overcoming this clinical challenge.

Depending on the physical barrier-scaffold material, GBR blocks surrounding soft tissue invasion, creates a certain space, and selectively guides stem cell differentiation to achieve bone tissue regeneration and repair bone defects (2). This technique has been widely used in oral periodontology and implantology. Ideal scaffold membranes prevent the interference of non-osteogenic tissue and provide space, mechanical support, and biological induction for bone regeneration; thus, these scaffolds directly impact GBR effects (3,4).

Numerous scaffold membranes classified as non-resorbable and bio-resorbable have been developed to serve a variety of functions in clinical applications. Non-resorbable scaffolds (5), such as nitrocellulose or expanded polytetrafluoroethylene (ePTFE), which require surgical removal after bone augmentation, are gradually being replaced by bio-resorbable GBR scaffold membranes, which have the advantages of excellent biocompatibility and absorbability and thus, no second surgery is needed. However, most existing absorbable scaffold membranes, including scaffolds composed of natural polymers, synthetic polymers, metallic materials, and inorganic polymers, have both advantages and disadvantages. For instance, collagen membranes of natural polymers come with fast degradation rates and a high risk for being contaminated (6), display insufficient strength to provide mechanical stability and lack osteoinductive properties. Most synthetic polymers, such as polycaprolactone (PCL) and polylactic acid (PLA), which exhibit hydrophobic behavior, low bioactivity, and long-term degradation *in vivo*, affect bone tissue regeneration (7-9). Metallic materials, such as titanium and cobalt-chromium alloys (6,10,11), have superior mechanical strength but also rigidity; they are too stiff and cannot be contoured easily; in addition, the sharp edges can perforate the soft tissue and subsequently expose the scaffold membrane. Ceramics with excellent biological properties, including hydroxyapatite (HA) and fluorapatite (FA), show weak mechanical stability, difficulty in shaping, and high brittleness, thus restricting their applications (12-14).

To overcome all the aforesaid challenges and integrate the advantages associated with different types of absorbable scaffold membranes, composite scaffolds, such as synthetic polymer/ceramic, have been fabricated. The basic requirement for all new composite scaffolds is the nanofibrous architecture, which is critically important for providing a 3D environment for cell and tissue ingrowth (15). Many fabrication processing techniques, including electrospinning and thermally induced phase separation, have been used to create nanofibrous scaffolds in bone tissue engineering (16,17). In previous study (18-20), electrospun polycaprolactone/FA (ePCL/FA) composite

---

Highlight box

Key findings
- Electrospun polycaprolactone incorporated with fluorapatite nanoparticles composite scaffolds enhance healing of experimental calvarial defect on rats.

What is known and what is new?
- The design of scaffolds is a critical consideration in bone tissue engineering. ePCL/FA composite scaffolds integrate the advantages of the bioactive fluorapatite and electrospun polycaprolactone.
- The fluorapatite crystal improved the hydrophilicity, and bioactivity of the ePCL/FA composite scaffolds.
- ePCL/FA composite scaffolds could repair the calvarial defect without negative effects *in vivo*.

What is the implication, and what should change now?
- ePCL/FA composite scaffolds demonstrate outstanding osteogenic potential for bone and orthopedic regenerative applications.

---

scaffold was successfully fabricated, in which the ePCL nanofiber scaffold provides a porous, hydrophilic and substantial three-dimensional network structure for cellular adaption, blood vessels formation and sufficient nutrient permission and FA acts as a mineralizing supplement to modifies the surface roughness of the 3D structure and creates mico- and nano-scale structures for providing greater protein adsorption, cell attachment and osteoblastic differentiation by surface coating technology.

ePCL/FA composite biomaterials without any added inductive promoting supplements have been regularly assessed for its osteoinductive and osteoconductive features with human dental pulp stem cells (DPSCs) (18), human mesenchymal stem cells (MSC) (13), and human adipose-derived stem cells (ASCs) (20). However, few studies have addressed the application of this scaffold membrane material *in vivo*. Here, the application and features of FA-modified ePCL scaffold *in vivo* and the possible mechanisms behind were preliminarily explored. We present this article in accordance with the ARRIVE reporting checklist (available at https://atm.amegroups.com/article/view/10.21037/atm-22-4865/rc).

Methods

Materials and fabrication of ePCL/FA composite scaffolds

A randomly oriented ePCL nanofiber scaffold was purchased from Nanofiber SOLUTIONS (Columbus, OH, USA) and the aforementioned ePCL nanofiber scaffold was soaked in an aqueous solution (pH 6.0, containing 0.10 mol/L HEDTA-Ca, 0.06 mol/L KH_2PO_4 and 0.02 mol/L KF) for the fabrication of the FA crystal coating. After incubation under biomimetic conditions of 37 ℃ and 1 standard atmosphere for 6, 12, 18, and 24 h, the final composite scaffold with the newly grown FA coating was rinsed with phosphate-buffered saline (PBS; GIBCO, Invitrogen), dried, sterilized by ultraviolet (UV) light, and stored in tight bottles until use. The synthesis and coating of FA crystals on ePCL nanofiber scaffolds were based on previous described procedures (18,20).

Characterization of ePCL and ePCL/FA scaffolds

After the pure ePCL and ePCL/FA scaffolds were fixed and sprayed with a conductive layer of Au, the nanofiber morphology and microstructure of the scaffold were viewed and digitally photographed using a LEO1530VP scanning electron microscope (SEM; Zeiss, Germany).

To evaluated the FA nanoparticle deposits on ePCL/FA composite scaffolds, X-ray diffraction (XRD) were performed. The Rigaku D/Max diffractometer was operated with a copper tube generated at a voltage of 40 kV and a current of 40 mA, set at a scan rate of 5°/min and 2θ range of 10°–70°.

To examine the effect of the synthesis time of the ePCL/FA scaffolds on the hydrophilic properties of the scaffolds, the water contact angles of ePCL and ePCL/FA were simultaneously measured at different time points. Under room temperature (RT), the water contact angles of the ePCL and ePCL/FA scaffold surfaces were measured with a Dropmaster 300 contact angle meter (Face-Kyowa, Dropmaster 300, Japan). The average contact angle was calculated based on at least three test points for each sample.

### Scaffold preparation and sterilization

The ePCL and ePCL/FA scaffold mats were trimmed with a hole puncher to a circular shape with a 5-mm diameter, depending on the size of the calvarial defect. The scaffolds were immersed in 75% volume/volume (v/v) ethanol/water solution for 30 minutes, and sterilized under UV light for 30 minutes on each side.

Experimental animals

Sixteen male Sprague-Dawley (SD) rats at 7-week-old, were maintained under specific pathogen-free conditions and provided with water and a standard laboratory diet ad libitum. After being fed adaptively for one week, all rats were randomly categorized into four groups: normal group (integral cranial structure without defect), control group (cranial defect), ePCL group (cranial defect repaired by electrospun polycaprolactone scaffolds), and ePCL/FA group (cranial defect repaired by FA-modified electrospun polycaprolactone scaffolds). All animal treatments and surgical procedures followed the protocols approved by the Animal Ethics Committee of Nanjing University (No. SYXK 2019-0056) and in accordance with the National Institutes of Health Guide for the Care and Use of Laboratory Animals.

Calvarial defect model

After anesthesia with pentobarbital sodium (0.25 mL/100 g body weight) via peritoneal injection, the rat with

Page 4 of 14

He et al. Composite scaffolds promote calvarial defect healing
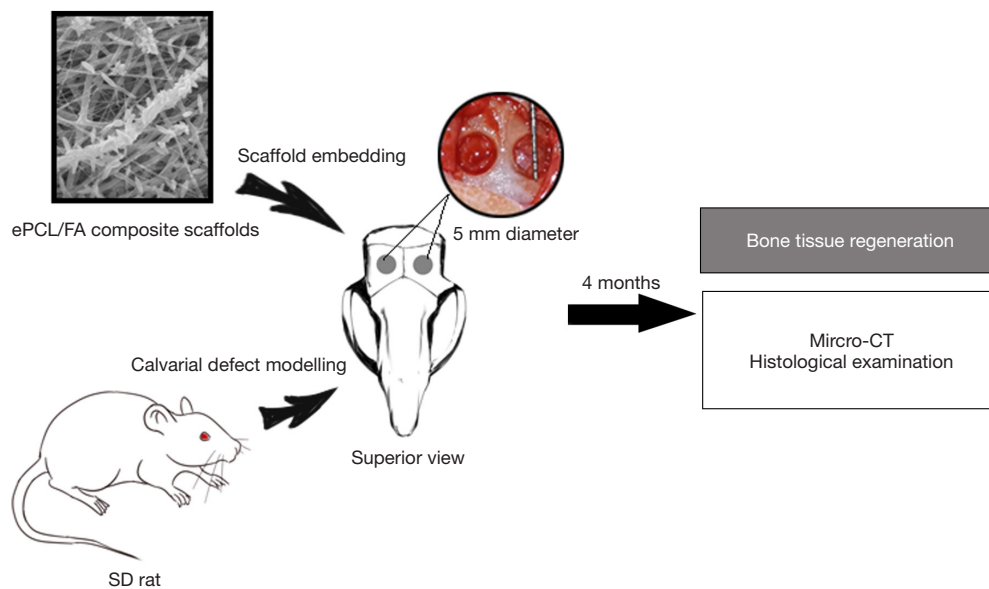
Figure 1 Schematic diagram of the rat calvarial defect experiment. ePCL, electrospun polycaprolactone; FA, fluorapatite; SD, Sprague-Dawley; micro-CT, micro-computed tomography.

experimental calvarial defect was created as reported previously (21-23). First, the skin was disinfected with 10% povidone-iodine solution, and then a 1% lidocaine and epinephrine (1:100,000) injection was performed subcutaneously under the surgical field. Then, a 1.5–2.0 cm horizontal incision was performed along the sagittal midline of the skull using a scalpel down to the periosteum, a self-retaining retractor was inserted to expose the calvarium, and calvarial defects with a diameter of 5 mm in the left and right skulls along the midline were symmetrically created by a surgical drill and trephine under saline irrigation. A full-thickness rectangular bone plate was gently elevated from the parietal bone to avoid damaging the dura mater and veins. In the normal group, a sham surgery was performed without defects. In the control group, cranial defects were repaired without scaffolds. In the ePCL and ePCL/FA groups, cranial defects were repaired using ePCL or ePCL/FA scaffolds. Finally, the surgical exposure was copiously washed with sterile normal saline and closed in three places using a simple interrupted 2-0 plain suture (Jinhuan, China). Penicillin was injected to prevent infection for three consecutive days after the operation.

Schematic illustrations of the procedures

After establishing the calvarial defect model, healing progressed uneventfully in all experimental animals and no postoperative complications were observed during the entire observation period. Schematic illustrations of the procedures for the construction and repair of calvarial defects in the SD rat model are shown in *Figure 1*.

Micro-computed tomography (micro-CT) analysis

At 1 week, 2 months, and 4 months after the surgery, we anesthetized the rats (n=4) via inhalation and performed an *in vivo* micro-CT examination of the calvarial defects. Micro-CT was carried out with a high-resolution SkyScan 1176 (Bruker, Germany) using a pixel size resolution of 18 μm, source voltage of 65 kV, and current of 385 μA. After scanning, three-dimensional virtual models of the region of interest (ROI) in the skulls were created and visualized using a micro view image processing software (CTvox software and DataViewer software). The ROI of the skull defect-related parameters was the surrounding bone area (diameter of 5 mm) at the center of the defect. Bone mineral density (BMD), bone volume (BV), tissue volume (TV), and bone volume percentage (BV/TV) were calculated using CTAn software. All data were presented as the mean ± standard deviation. The raw data supporting the findings of this study are available from the corresponding author upon reasonable request.
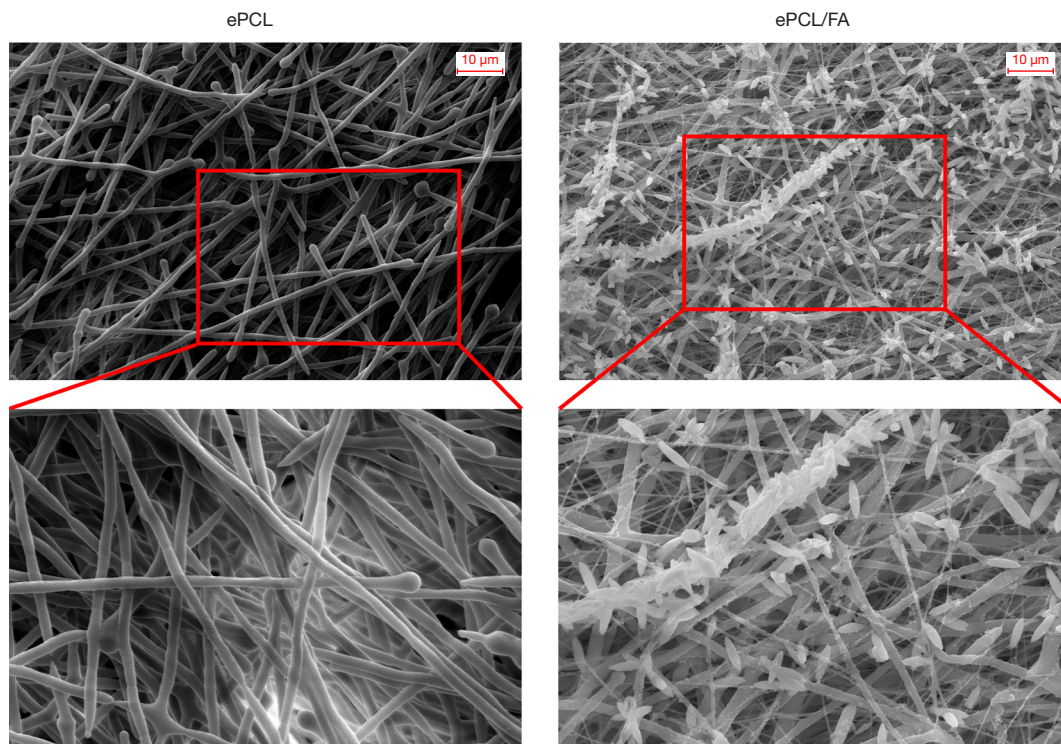
Figure 2 The morphology of composite scaffolds. SEM images of ePCL and ePCL/FA. Scale bar: 10 µm. ePCL, electrospun polycaprolactone; FA, fluorapatite; SEM, scanning electron microscope (Zeiss, Germany).

Histological analysis

Four months after the operation, all animals were euthanized to prepare specimens for analysis in accordance with the animal experimental ethical standards of Nanjing University. Skull specimens were hemisected and fixed with 4% paraformaldehyde. After decalcification, dehydration, and embedding in paraffin, the specimens were sliced into 4 µm sections. These sections were then stained with hematoxylin and eosin (H&E), Van Gieson (VG), and Masson stains.
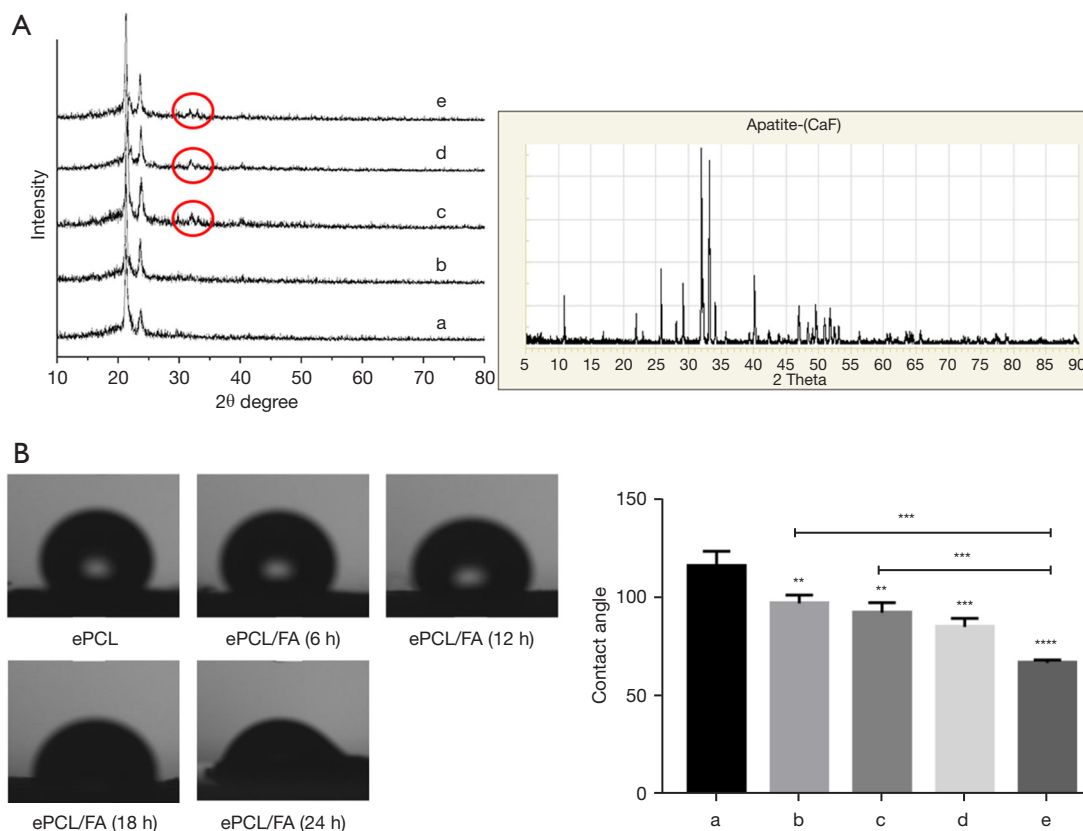
Statistical analysis

Data were analyzed using GraphPad Prism software (version 6.0; GraphPad Software, San Diego, CA, USA). All data were expressed as the mean ± standard deviation. Statistical differences between experimental variants, including BMD, BV, TV BV/TV percentage and water contact angles, were determined using a one-way analysis of variance, followed by Tukey's multiple comparisons test to compare individual groups. A P value of less than 0.05 indicated statistical significance.

Results

Morphological structure, XRD and water contact angle

As well known, that the design of scaffolds is a critical consideration in bone tissue engineering. To observe the morphological structures of the ePCL and ePCL/FA composite scaffolds, the samples were carefully studied via scanning electron microscopy. As shown in the SEM images (*Figure 2*), each scaffold group had a micro/nanoscale topology. The surface of the ePCL nanofiber scaffolds was smooth and uniform, while the interior of the ePCL was arranged in a disordered manner to form an interwoven and porous three-dimensional network structure. The FA crystals were uniformly distributed on the fiber surface and micropores in granular form in the ePCL/FA composite scaffolds.

XRD, was employed to further characterize the physicochemical properties of ePCL/FA composite scaffolds, specifically the FA nanoparticle deposits. *Figure 3A* shows the XRD patterns of each group and the standard diffraction cards of pure FA samples (JCPDS 15-0876). Compared with the FA standard diffraction card, it was

Ann Transl Med 2023;11(9):313 | https://dx.doi.org/10.21037/atm-22-4865

Page 6 of 14

He et al. Composite scaffolds promote calvarial defect healing

Figure 3 Characterization of composite scaffolds. (A) X-ray diffraction spectra of FA in the composite samples and the standard diffraction cards of pure FA. Peaks of interests are designated by red circles. (B) Contact angle of each group, including the (a) ePCL and (b-e) ePCL/FA composite scaffolds at the different synthesis time points (6, 12, 18 and 24 h). **, P<0.01; ***, P<0.001; ****, P<0.0001. ePCL, electrospun polycaprolactone; FA, fluorapatite.

found that the diffraction peak (shown in the red circle) was obvious with the change of synthesis time, which indicating that crystalline FA structures present in the composites (12, 18, 24 h) as opposed to the completely amorphous nature of ePCL scaffolds.

The surface hydrophilic properties of biomaterials influence the attachment and proliferation of different cells. The water contact angle of the material was measured to evaluate its wettability, with a contact angle below or above 90° indicating hydrophilicity and hydrophobicity, respectively. *Figure 3B* summarizes the contact angle measurements performed on the pure ePCL and ePCL/ FA composite scaffolds at different synthesis times (6, 12, 18 and 24 h). For the pure ePCL nanofibers, the average contact angle was greater than 100°. For the ePCL/FA group, the water contact angle was significantly decreased compared with that of the ePCL group (P<0.05) and gradually decreased with an increase in synthesis time,

indicating higher hydrophilicity.

Hence, these results indicated that PCL could be fabricated by electrospinning into a hydrophobic nanofibrous scaffold with a three-dimensional network structure similar to that of the extracellular matrix, and it could be modified by adding mineralization supplements, namely, FA crystals, to form an excellent hydrophilic biocomposite scaffold.

Micro-CT imaging examination and results

One week after the surgery, all animals exhibited normal behavior without any limitations compared with the preoperative values. Micro-CT was performed to detect and analyze their skull defects, and the results were used as the original data for skull defect modelling. The 3D reconstructed images clearly demonstrated calvarial defects in the control, ePCL, and ePCL/FA groups without any

bone formation (*Figure 4A*).

Meanwhile, the BMD, BV, TV, and BV/TV percentage surrounding the ROI were also measured at 1 week, 2 months, and 4 months after surgery (*Figure 4B*). It was observed that the critical-sized calvarial defect model was successfully established in the SD rats and caused loss of bone quality around the detected areas with minimal regeneration over time (control group). Implantation of pure ePCL resulted in insignificant new bone reconstruction and a negligible increase in bone quality. In contrast, implantation with ePCL/FA groups led to the filling of skull defects with mineralized tissue and remarkable increases in bone quality (including BMD, BV, and BV/TV percentage) compared to those in the control and ePCL groups (P<0.05) at the same time points (2 and 4 months).

Histology examination

Histological images of HE, VG, and Masson staining were prepared for all groups at 4 months. H&E staining revealed an integral and mature cranial structure without defects in the normal group, a small amount of new bone only at the edge region adjacent to the original bone in the control group, and relatively less irregular new bone in the borderline and center of the defect and discontinuous results in the ePCL group. Compared with the aforementioned new bone in the control and ePCL groups, the ePCL/FA group showed more continuous, complete, and mature results and exhibited a layered structure. With the ePCL/FA treatment, the calvarial defects showed the formation of pink homogeneous bone tissue (red arrow), that is, the calvarial defects were regeneratively repaired (*Figure 5*).

Masson and VG staining indicate the elastic and collagenous fibers in the calvarial defect area. Masson staining showed a large amount of dark red continuous bone tissue with blood vessels in the ePCL/FA groups, suggesting that mature bone tissue formed in the defect area. In the control group, the marginal area of the bone defect was occupied by dark red homogeneously stained bone tissue, and the rest of the defect area was occupied by a large amount of navy blue and light red fibrous connective tissue. In the ePCL groups, blue and light red fibrous connective tissues covered the entire bone defect region (*Figure 6*).

VG staining showed a large amount of vermilion homogeneous bone collagen tissue and a small amount of yellow fibrous connective tissue in the ePCL/FA group, suggesting that mature bone tissue and new collagen tissue had formed. In the control group, the bone defect area was occupied by half vermilion homogeneously stained bone collagen tissue and half yellow fibrous connective tissue. In the ePCL groups, fibrous connective tissue covered the whole bone defect region and relatively less homogeneously stained bone collagen tissue was observed in the borderline of the defect (*Figure 7*).

Discussion

Critical bone tissue defects that exceed the self-healing capacity of bone often require xenografts or autologous bone grafts (24,25). The development of GBR using osteoinductive and conductive scaffold materials may offer an alternative approach to overcoming this problem (26-28). However, different types of biomaterials that represent basic components of scaffolds have their own advantages and disadvantages; therefore, we attempted to fabricate composite scaffold membranes to maximize their benefits. In our previous study, ePCL/FA composite scaffolds were successfully fabricated (18-20).

PCL is a synthetic biodegradable polymer with high mechanical strength, flexibility, biocompatibility, and biodegradability, and it has been approved by the U.S. Food and Drug Administration (FDA) and widely studied in the fields of tissue engineering and bone healing materials (29-31). As well known, that the design of scaffolds is a critical consideration in bone tissue engineering. Electrospinning technology (32,33), is considered an efficient method of converting PCL into nanofiber scaffolds with nanomicron three-dimensional porous structures. However, PCL nanofiber scaffold membranes have a weak osteoinductive effect and a hydrophobic nature (9). Thus, research has focused on reinforced nanocomposite scaffold membranes modified by surface coating with mineralization-inducing supplements, such as ceramics.

HA and its composites, as common bioceramic materials, represent the most common form of bone mineral and provide mechanical strength and significant osteoinductive properties (34). However, because HA has a certain solubility in biological fluids and can be decomposed when heated, its long-term stability is poor (35). FA is a bioactive and biocompatible ceramic that is structurally and chemically similar to HA, and it presents high chemical stability. In addition, FA has much lower solubility in biological fluids than HA and presents excellent osteoinductive effects and antibacterial ability (36,37). Our research group used FA crystals as a coating on the surface of ePCL nanofibers to optimize their surface microstructure

Page 8 of 14

He et al. Composite scaffolds promote calvarial defect healing
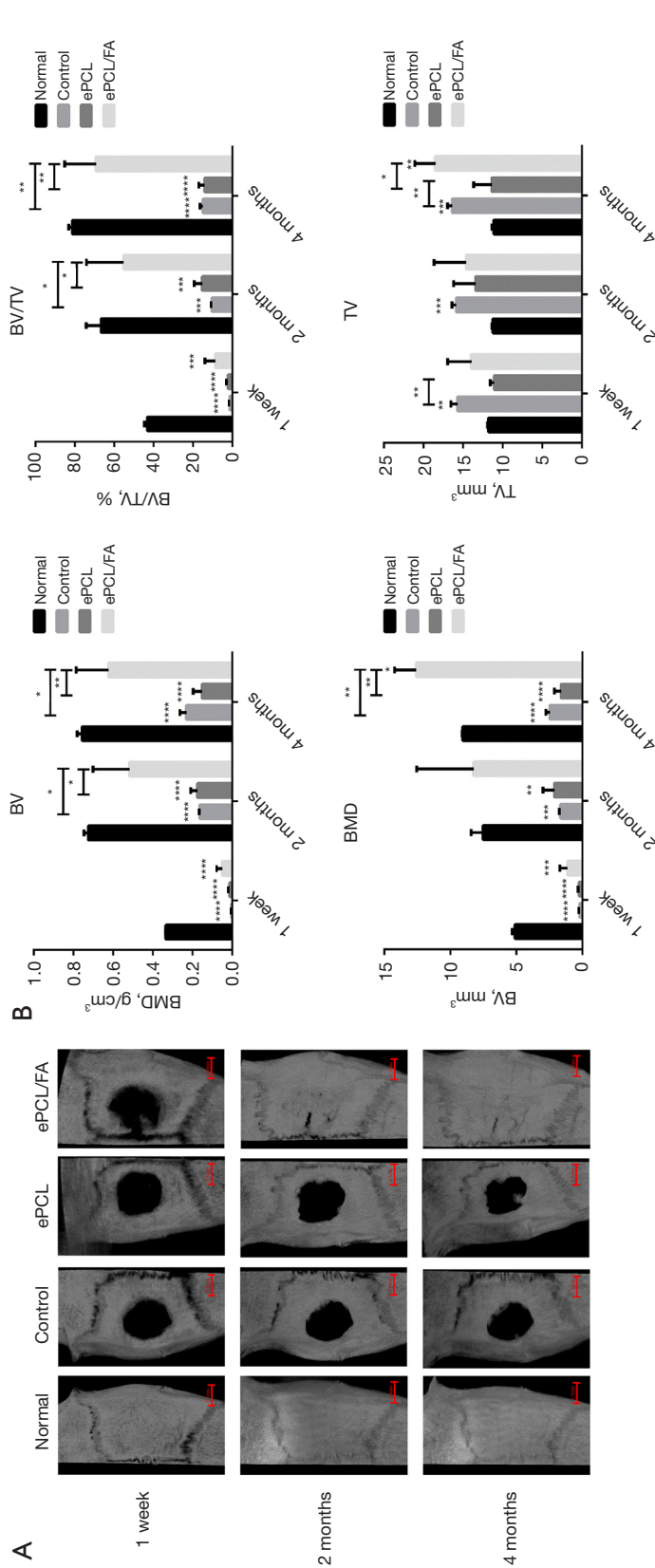
Figure 4 Micro-CT images and analysis of the repair of the rat calvarial defect. (A) 3D reconstructed digitized images at 1 week, 2 months, and 4 months. (B) Bone-related parameters (BMD, BV, TV, and BV/TV percentage). *, P<0.05; **, P<0.01; ***, P<0.001; ****, P<0.0001. Normal group (integral cranial structure without defect); control group (cranial defect); ePCL group (cranial defect repaired by electrospun polycaprolactone scaffolds); and ePCL/FA group (cranial defect repaired by fluorapatite-modified electrospun polycaprolactone scaffolds). ePCL, electrospun polycaprolactone; FA, fluorapatite; BMD, bone mineral density; BV, bone volume; TV, tissue volume; BV/TV, bone volume percentage; micro-CT, micro-computed tomography.
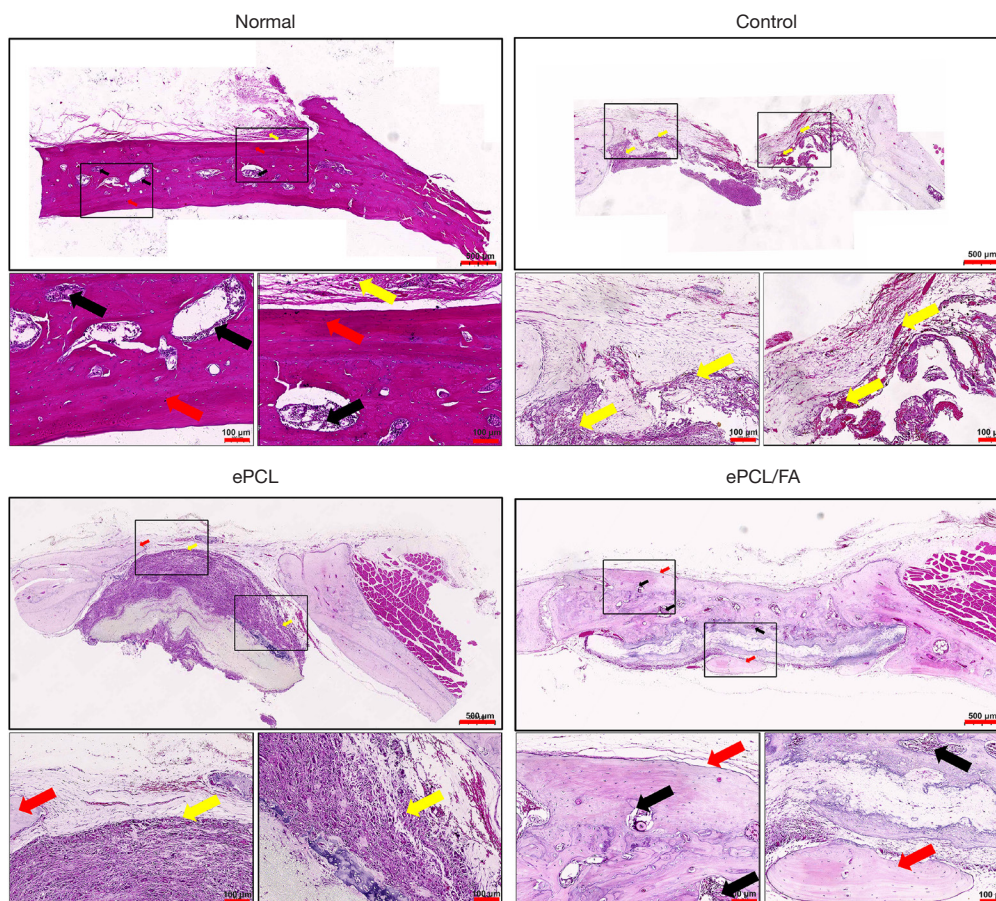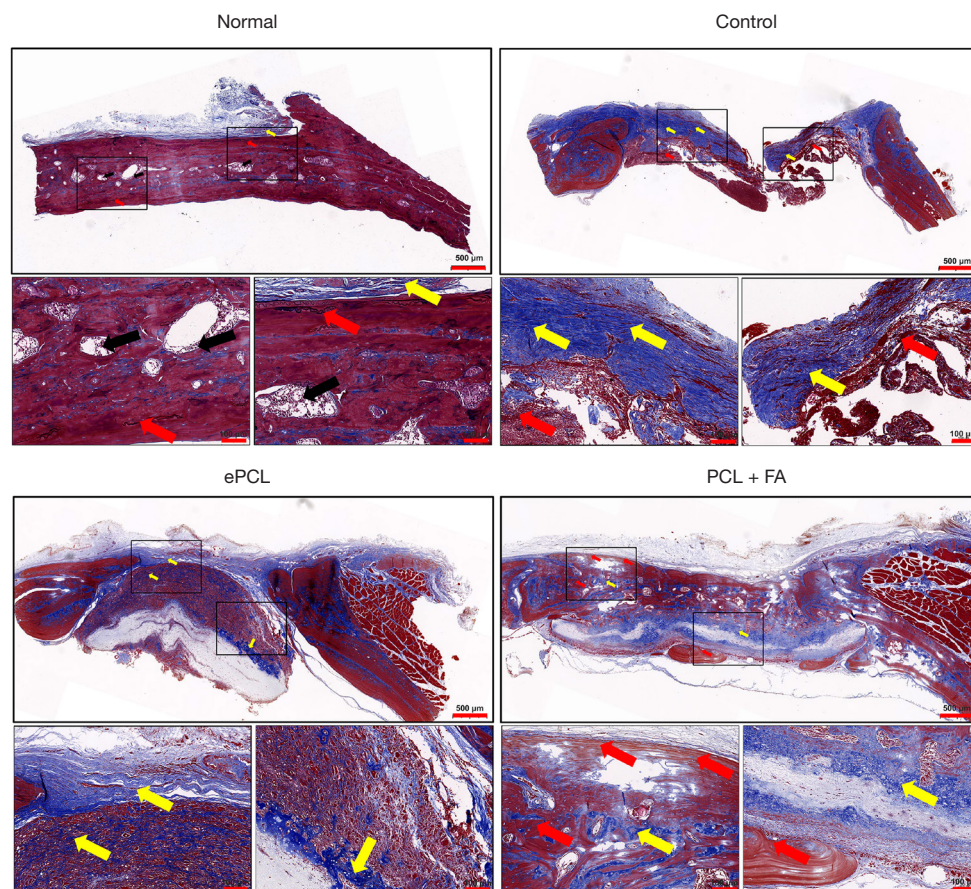
Figure 5 H&E staining of the four groups at 4 months. The 2 small boxes below are high-magnification images of the indicated portion in the above box. Red arrows indicate bone tissue, yellow arrows indicate fibrous connective tissue, and black arrows indicate blood vessel. Scale bar: 500 µm (up); 100 µm (down). ePCL, electrospun polycaprolactone; FA, fluorapatite; H&E, hematoxylin and eosin.

and osteoinductive ability. According to SEM images (*Figure 2*), the FA nanoparticles were uniformly distributed on the fiber surface and micropores in granular form in the ePCL/FA composite scaffolds, which is essential for the improvement of mechanical and biological properties of the scaffolds. As additional evidence for the presence of FA nanoparticle in ePCL/FA composite scaffolds, XRD approach was employed. These distinct peaks in *Figure 3A* indicate introduction of crystalline properties into the amorphous nanostructure of the ePCL/FA composite scaffolds due to the presence of FA and, therefore, indicate the formation of a biocomposite material. In addition, a series of *in vitro* experiments demonstrated that the ePCL/FA composite scaffolds have good biocompatibility and outstanding potential for osteoinduction and osteoconduction of DPSCs and human periodontal ligament cells (18,20,38). The hydrophilicity of the biomaterial plays

an important role in bone tissue engineering by modulating osteogenic cell attachment, proliferation and differentiation for (39). As shown in *Figure 3B*, it was found that the ePCL/FA composite scaffolds improved hydrophilicity to overcome the inherent hydrophobicity of the pure ePCL polymer, which could be attributed to the increased surface area of the ePCL nanofibers owing to the existence of submicron structures on the surface in the presence of FA nanoparticles.

All studies demonstrated that incorporating FA nanoparticles into the ePCL scaffold improved the osteoinductive and osteoconductive properties as well as the wettability of the scaffold, which are insufficient in pure ePCL materials. Therefore, ePCL/FA composite scaffolds represent a biomaterial composite for possible application in bone tissue engineering; however, comprehensive evaluations of its potential based on *in vivo* studies are

Page 10 of 14

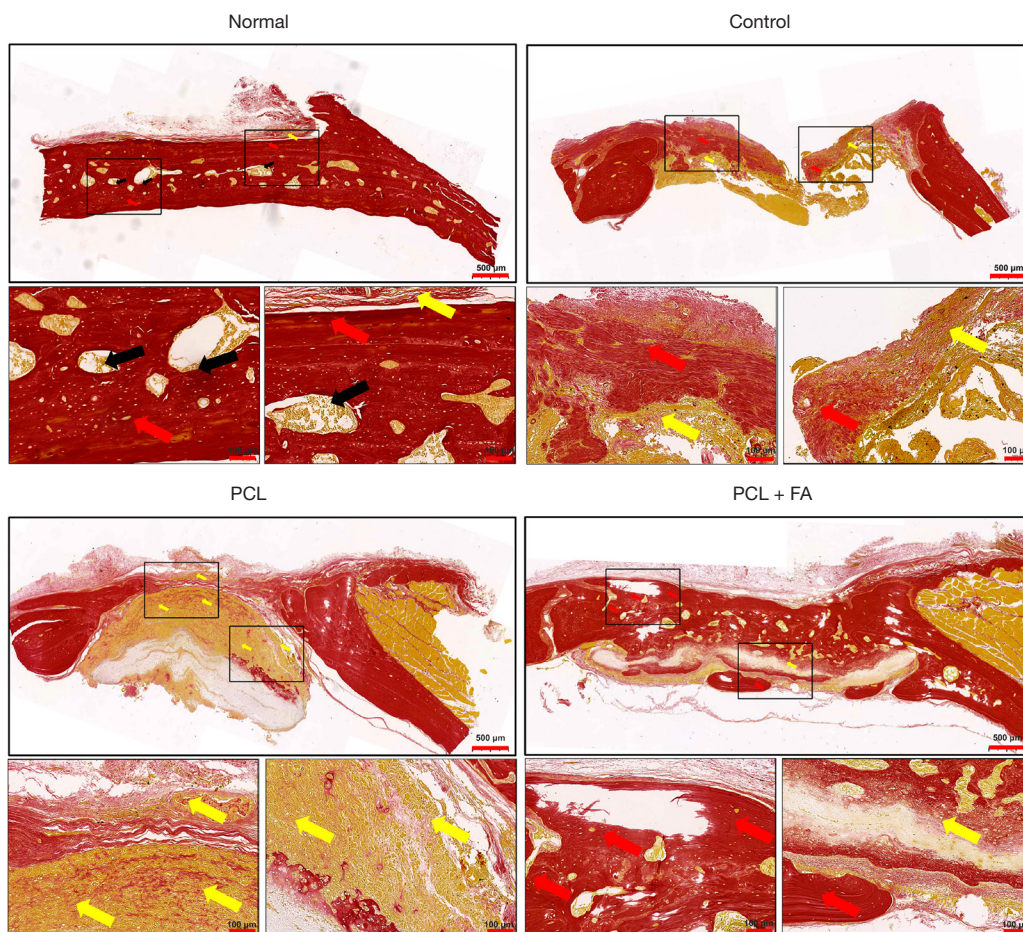He et al. Composite scaffolds promote calvarial defect healing

Figure 6 Masson staining of the four groups at 4 months. The 2 small boxes below present high-magnification images of the indicated portion in the above box. Red arrows indicate bone tissue, yellow arrows indicate fibrous connective tissue, and black arrows indicate blood vessel. Scale bar: 500 μm (up); 100 μm (down). ePCL, electrospun polycaprolactone; FA, fluorapatite.

still required. Animal models are key to the preclinical development of translational technologies. Several small animal models had been developed for bone tissue engineering (40,41). Here in this study, a rat calvarial defect model was introduced, which was economical, practical, and reproducible and could reliably simulate the pathological state of bone defects for the evaluation of biomaterials and bone tissue engineering technologies.

In the current study, the results of micro-CT and histology showed that the 5-mm diameter calvarial defects did not heal without intervention in the control group after 4 months, pure ePCL also failed to repair the defect, while the ePCL/FA composite scaffolds could repair the calvarial defect completely after 4 months. This indicated that a critical-size calvarial defect was successfully modelled and the hydrophilized ePCL/FA composite scaffolds show outstanding osteogenic potential for bone and orthopedic

regenerative applications without negative effects *in vivo*. Interestingly, in the case of Masson and VG staining (*Figures 6*,*7*), the pure ePCL group appeared to have less bone collagen tissue covering the whole bone defect region than the pure cranial defect group (control group). A possible reason behind this phenomenon is that the pure ePCL scaffolds failed to promote osteoinduction by the proliferation of bone cells owing to their hydrophobic nature. Furthermore, considerable fibrous connective tissue formed at the interface of the calvarial defects, resulting in a fibrous tissue capsule that prevented osteointegration and ultimately caused regeneration failure in the ePCL group.

The newly developed ePCL/FA composite scaffolds have been well validated *in vitro* (DPSCs and hPDLCS) and *in vivo* (rat calvarial defect model), and they promote bone regeneration and reconstruction. However, in clinical practice, the healing of bone defects is carried out in an

Figure 7 VG staining of the four groups at 4 months. The 2 small boxes below present high-magnification images of the indicated portion in the above box. Red arrows indicate bone tissue, yellow arrows indicate fibrous connective tissue, and black arrows indicate blood vessel. Scale bar: 500 µm (up); 100 µm (down). PCL, polycaprolactone; FA, fluorapatite; VG, Van Gieson.

infected and load-bearing environment, which requires scaffold materials that can induce osteogenesis and present good anti-inflammatory effects and mechanical stability. Therefore, in future experiments, the ePCL/FA composite scaffolds in a more complex bone defect environment will be further investigated, such as periodontal fenestration defect and intrabony defect models, to obtain desirable features of scaffold materials that can complete clinical translation.

Conclusions

In summary, this study is the first to investigate the application of ePCL/FA composite scaffolds for bone tissue regeneration *in vivo*. In the clinical transformation of ePCL/FA, it was demonstrated that the FA crystal modified

the biocompatibility, hydrophilicity, and osteoinductive properties of ePCL. Moreover, the cranial defects were almost completely repaired by ePCL/FA composite scaffolds at 4 months compared with the control and ePCL groups. These findings indicate that ePCL/FA synthetic scaffolds possess great potential for bone tissue regeneration.

Acknowledgments

Page 12 of 14

He et al. Composite scaffolds promote calvarial defect healing

Footnote

Reporting Checklist: The authors have completed the ARRIVE reporting checklist. Available at https://atm.amegroups.com/article/view/10.21037/atm-22-4865/rc

Data Sharing Statement: Available at https://atm.amegroups.com/article/view/10.21037/atm-22-4865/dss

Peer Review File: Available at https://atm.amegroups.com/article/view/10.21037/atm-22-4865/prf

Conflicts of Interest: All authors have completed the ICMJE uniform disclosure form (available at https://atm.amegroups.com/article/view/10.21037/atm-22-4865/coif). The authors have no conflicts of interest to declare.

Ethical Statement: The authors are accountable for all aspects of the work in ensuring that questions related to the accuracy or integrity of any part of the work are appropriately investigated and resolved. All animal treatments and surgical procedures followed the protocols approved by the Animal Ethics Committee of Nanjing University (No. SYXK 2019-0056) and in accordance with the National Institutes of Health Guide for the Care and Use of Laboratory Animals.

References

1. Gao R, Watson M, Callon KE, et al. Local application of lactoferrin promotes bone regeneration in a rat critical-sized calvarial defect model as demonstrated by micro-CT and histological analysis. J Tissue Eng Regen Med 2018;12:e620-6.

2. Omar O, Elgali I, Dahlin C, et al. Barrier membranes: More than the barrier effect? J Clin Periodontol 2019;46 Suppl 21:103-23.

3. Zhang X, Chen X, Hong H, et al. Decellularized extracellular matrix scaffolds: Recent trends and emerging strategies in tissue engineering. Bioact Mater 2022;10:15-31.

4. Du Y, Guo JL, Wang J, et al. Hierarchically designed bone scaffolds: From internal cues to external stimuli. Biomaterials 2019;218:119334.

5. Gentile P, Chiono V, Tonda-Turo C, et al. Polymeric membranes for guided bone regeneration. Biotechnol J 2011;6:1187-97.

6. Ren Y, Fan L, Alkildani S, et al. Barrier Membranes for Guided Bone Regeneration (GBR): A Focus on Recent Advances in Collagen Membranes. Int J Mol Sci 2022;23:14987.

7. Coenen AMJ, Bernaerts KV, Harings JAW, et al. Elastic materials for tissue engineering applications: Natural, synthetic, and hybrid polymers. Acta Biomater 2018;79:60-82.

8. Adithya SP, Sidharthan DS, Abhinandan R, et al. Nanosheets-incorporated bio-composites containing natural and synthetic polymers/ceramics for bone tissue engineering. Int J Biol Macromol 2020;164:1960-72.

9. de Siqueira L, Ribeiro N, Paredes MBA, et al. Influence of PLLA/PCL/HA Scaffold Fiber Orientation on Mechanical Properties and Osteoblast Behavior. Materials (Basel) 2019;12:3879.

10. Wang X, Wang G, Zhao X, et al. Short-Term Evaluation of Guided Bone Reconstruction with Titanium Mesh Membranes and CGF Membranes in Immediate Implantation of Anterior Maxillary Tooth. Biomed Res Int 2021;2021:4754078.

11. Decco O, Cura A, Beltrán V, et al. Bone augmentation in rabbit tibia using microfixed cobalt-chromium membranes with whole blood, tricalcium phosphate and bone marrow cells. Int J Clin Exp Med 2015;8:135-44.

12. Taktak R, Elghazel A, Bouaziz J, et al. Tricalcium phosphate-Fluorapatite as bone tissue engineering: Evaluation of bioactivity and biocompatibility. Mater Sci Eng C Mater Biol Appl 2018;86:121-8.

13. Malysheva K, Kwaśniak K, Gnilitskyi I, et al. Functionalization of Polycaprolactone Electrospun Osteoplastic Scaffolds with Fluorapatite and Hydroxyapatite Nanoparticles: Biocompatibility Comparison of Human Versus Mouse Mesenchymal Stem

Cells. Materials (Basel) 2021;14:1333.

14. Borkowski L, Przekora A, Belcarz A, et al. Fluorapatite ceramics for bone tissue regeneration: Synthesis, characterization and assessment of biomedical potential. Mater Sci Eng C Mater Biol Appl 2020;116:111211.

15. Holzwarth JM, Ma PX. Biomimetic nanofibrous scaffolds for bone tissue engineering. Biomaterials 2011;32:9622-9.

16. Muthukrishnan L. An overview on electrospinning and its advancement toward hard and soft tissue engineering applications. Colloid Polym Sci 2022;300:875-901.

17. Miszuk JM, Hu J, Sun H. Biomimetic Nanofibrous 3D Materials for Craniofacial Bone Tissue Engineering. ACS Appl Bio Mater 2020;3:6538-45.

18. Guo T, Li Y, Cao G, et al. Fluorapatite-modified scaffold on dental pulp stem cell mineralization. J Dent Res 2014;93:1290-5.

19. Guo T, Cao G, Li Y, et al. Signals in Stem Cell Differentiation on Fluorapatite-Modified Scaffolds. J Dent Res 2018;97:1331-8.

20. Li Y, Guo T, Zhang Z, et al. Autophagy Modulates Cell Mineralization on Fluorapatite-Modified Scaffolds. J Dent Res 2016;95:650-6.

21. Ikumi R, Miyahara T, Akino N, et al. Guided bone regeneration using a hydrophilic membrane made of unsintered hydroxyapatite and poly(L-lactic acid) in a rat bone-defect model. Dent Mater J 2018;37:912-8.

22. Spicer PP, Kretlow JD, Young S, et al. Evaluation of bone regeneration using the rat critical size calvarial defect. Nat Protoc 2012;7:1918-29.

23. Kim KS, Lee JY, Kang YM, et al. Small intestine submucosa sponge for in vivo support of tissue-engineered bone formation in the presence of rat bone marrow stem cells. Biomaterials 2010;31:1104-13.

24. Vidal L, Brennan MÁ, Krissian S, et al. In situ production of pre-vascularized synthetic bone grafts for regenerating critical-sized defects in rabbits. Acta Biomater 2020;114:384-94.

25. Schmidt AH. Autologous bone graft: Is it still the gold standard? Injury 2021;52 Suppl 2:S18-22.

26. Papageorgiou SN, Papageorgiou PN, Deschner J, et al. Comparative effectiveness of natural and synthetic bone grafts in oral and maxillofacial surgery prior to insertion of dental implants: Systematic review and network meta-analysis of parallel and cluster randomized controlled trials. J Dent 2016;48:1-8.

27. Lohmann P, Willuweit A, Neffe AT, et al. Bone regeneration induced by a 3D architectured hydrogel in a rat critical-size calvarial defect. Biomaterials 2017;113:158-69.

28. Tu C, Bajwa A, Shi A, et al. Effect of fibrin glue on the healing efficacy of deproteinized bovine bone and autologous bone in critical-sized calvarial defects in rats. Clin Oral Investig 2022;26:2491-502.

29. Dwivedi R, Kumar S, Pandey R, et al. Polycaprolactone as biomaterial for bone scaffolds: Review of literature. J Oral Biol Craniofac Res 2020;10:381-8.

30. Malikmammadov E, Tanir TE, Kiziltay A, et al. PCL and PCL-based materials in biomedical applications. J Biomater Sci Polym Ed 2018;29:863-93.

31. Joo G, Sultana T, Rahaman S, et al. Polycaprolactone-gelatin membrane as a sealant biomaterial efficiently prevents postoperative anastomotic leakage with promoting tissue repair. J Biomater Sci Polym Ed 2021;32:1530-47.

32. Wang T, Ji X, Jin L, et al. Fabrication and characterization of heparin-grafted poly-L-lactic acid-chitosan core-shell nanofibers scaffold for vascular gasket. ACS Appl Mater Interfaces 2013;5:3757-63.

33. Zhao H, Tang J, Zhou D, et al. Electrospun Icariin-Loaded Core-Shell Collagen, Polycaprolactone, Hydroxyapatite Composite Scaffolds for the Repair of Rabbit Tibia Bone Defects. Int J Nanomedicine 2020;15:3039-56.

34. Granito RN, Muniz Renno AC, Yamamura H, et al. Hydroxyapatite from Fish for Bone Tissue Engineering: A Promising Approach. Int J Mol Cell Med 2018;7:80-90.

35. Mohd Roslan MR, Mohd Kamal NL, Abdul Khalid MF, et al. The State of Starch/Hydroxyapatite Composite Scaffold in Bone Tissue Engineering with Consideration for Dielectric Measurement as an Alternative Characterization Technique. Materials (Basel) 2021;14:1960.

36. Jeyapalina S, Hillas E, Beck JP, et al. Fluorapatite and fluorohydroxyapatite apatite surfaces drive adipose-derived stem cells to an osteogenic lineage. J Mech Behav Biomed Mater 2022;125:104950.

37. Wang X, Zhang Z, Chang S, et al. Fluorapatite enhances mineralization of mesenchymal/endothelial cocultures. Tissue Eng Part A 2014;20:12-22.

38. Ren S, Yao Y, Zhang H, et al. Aligned Fibers Fabricated by Near-Field Electrospinning Influence the Orientation and Differentiation of hPDLSCs for Periodontal Regeneration. J Biomed Nanotechnol 2017;13:1725-34.

39. Xing Z, Cai J, Sun Y, et al. Altered Surface Hydrophilicity on Copolymer Scaffolds Stimulate the Osteogenic Differentiation of Human Mesenchymal Stem Cells. Polymers (Basel) 2020;12:1453.

40. Kotagudda Ranganath S, Schlund M, Delattre J, et al. Bilateral double site (calvarial and mandibular) critical-

Page 14 of 14

He et al. Composite scaffolds promote calvarial defect healing

size bone defect model in rabbits for evaluation of a craniofacial tissue engineering constructs. Mater Today Bio 2022;14:100267.

41. Wu D, Wang Z, Zheng Z, et al. Effects of physiological aging factor on bone tissue engineering repair based on fetal BMSCs. J Transl Med 2018;16:324.